Accepted Manuscript

Late Quaternary tectonic activity and crustal shortening rate of the Bogda mountain area, eastern Tian Shan, China

Chuanyong Wu, Guodong Wu, Jun Shen, Xunye Dai, Jianbo Chen, Heping Song

PII: S1367-9120(16)30001-3
DOI: http://dx.doi.org/10.1016/j.jseaes.2016.01.001
Reference: JAES 2606

To appear in: *Journal of Asian Earth Sciences*

Received Date: 11 July 2015
Revised Date: 30 December 2015
Accepted Date: 4 January 2016

Please cite this article as: Wu, C., Wu, G., Shen, J., Dai, X., Chen, J., Song, H., Late Quaternary tectonic activity and crustal shortening rate of the Bogda mountain area, eastern Tian Shan, China, *Journal of Asian Earth Sciences* (2016), doi: http://dx.doi.org/10.1016/j.jseaes.2016.01.001

Late Quaternary tectonic activity and crustal shortening rate of the Bogda mountain area, eastern Tian Shan, China

Chuanyong Wu[1,2], Guodong Wu[2], Jun Shen[3], Xunye Dai[3], Jianbo Chen[2], Heping Song[2]

1. State Key Laboratory of Earthquake Dynamics, Institute of Geology, CEA, Beijing 100029

2. Seismological Bureau of Xinjiang Uygur Autonomous Region, Urumqi 830011

3. Institute of Disaster Prevention, Langfang 101601

Abstract: The Bogda mountain range is the highest range among the northern Tian Shan mountains. Based on geologic and geomorphologic field surveys, trench excavation and optically stimulated luminescence (OSL) dating, we targeted the active Fukang fault along the Bogda mountain range and identified the late Quaternary deformation characteristics of this area. We found that the Fukang fault dislocated different geomorphic surfaces of the northern Bogda piedmont. The vertical fault displacement corresponds to the topographic relief of the Bogda over long time scales. Since the late Quaternary, the crustal shortening rate was estimated to be 0.90±0.20 mm/yr, which is less than that of the western segment of the northern Tian Shan. We interpret the Bogda fold and thrust belt to be a thick-skinned structure, since a high angle thrust fault bounds the Bogda mountain range and the foreland basin. The deformation characteristics of this region have been dominated by vertical uplift, and the component of propagation towards the basin has been very limited. This tectonic deformation is evidenced as vertical growth. Although the deformation rate is small, the uplift amplitude is very significant in this region.

Keywords: Bogda mountain, Late Quaternary, crustal shortening rate, tectonic

deformation

1. Introduction

The Tian Shan (Shan is mountain in Chinese) is bounded by the Tarim basin to the south and the Junggar basin and Kazakh platform to the north (Fig. 1). It is 2,500 km long from east to west and approximately 250-350 km wide from north to south. Reactivation of the Tian Shan orogenic belt during the Cenozoic has been considered to have resulted from the remote effects of the India-Eurasia collision (Molnar and Tapponnier, 1975; Tapponnier and Molnar, 1979; Hendrix et al., 1994; Yin et al., 1998; Deng et al., 2000; Zhang et al., 2003).

Present-day GPS measurements indicate the crustal shortening rate is approximately 20 mm/yr across the western Tian Shan (Abdrakhmatov et al.,1996; Reigber et al., 2001; Wang et al., 2002; Zhang et al., 2002; Yang et al., 2008; Zubovich et al., 2010). Further, all of the geological, numerical, and GPS observations indicate that the tectonic deformation of the Tian Shan is characterized by a gradual decaying trend from west to east (Avouac et al.,1993; Reigber et al., 2001; Zhang et al., 2002). Near the Bogda area, the crustal shortening rate is only 1-2 mm/yr (Li et al., 2010; Yang et al., 2008). In the Hami area, the crustal shortening rate approaches 0 (Zhang et al., 2002). The topography also shows the same characteristics, with a series of >5000 m peaks in the western Tian Shan and a series of <2000 m peaks in the eastern Tian Shan (Fig. 1).

There are four main nappe structures in the piedmont of the Tian Shan mountains (Deng et al., 2000). Except for the Bogda arcuate nappe structure, the other three

structural systems have all been responsible for strong earthquakes with magnitude of 7 or 8 through history (Fig. 1). In the Bogda area, no strong earthquake (with a magnitude greater than 7) has been recorded, and moderate earthquakes in this region are also rare compared with the other nappe structures. In contrast, the tectonic uplift of this area is very intense. Bogda peak, with an elevation of 5445 m, is the highest peak in the northern Tian Shan. It is obvious that the seismic activity is not in agreement with the tectonic geomorphology. The Bogda range has been uplifted since the Miocene following the India-Eurasia collision (Tapponnier and Molnar, 1979; Hendrix et al., 1994; Deng et al., 2000). Apatite fission track data indicate that the main uplift stage of the Bogda mountain range was after the Neogene (Wang et al., 2008). Since the geomorphology of the Bogda area is significantly different from the eastern Tian Shan, questions regarding these differences remain. In addition, the deformation features of this area also need to be explored and discussed.

To reveal the tectonic characteristics of the Bogda area and the late Quaternary kinematic features of the fault, we report here our geological and geomorphological field survey observations, including terrace deformation measurements, trench excavation and optically stimulated luminescence (OSL) dating. Furthermore, we will discuss the active characteristics of the main fault since the late Quaternary. Then, combined with the deep structure of the Bogda region, we will generalize and discuss the characteristics of tectonic deformation around the Bogda range area.

2. Geology and seismicity of the Bogda mountain range

Cenozoic tectonic deformation of the Tian Shan is characterized by expansion

both to the north and south sides and development of reverse fault and fold belts (Avouac et al., 1993; Liu et al., 1994; Zhang et al., 1996; Abdrakhmatov et al., 1996; Ghose et al., 1998; Allen et al., 1999; Burbank et al., 1999; Burchfiel et al., 1999; Deng et al., 2000; Fu et al., 2003). These nappe structures are the most intense regions of tectonic deformation, and the strongest earthquakes have occurred along these structures (Yang et al., 2008).

The Bogda fold and thrust belt is an arched anticlinorium that is bounded by the Junggar basin to the north and the Chaiwopu depression to the south (Fig. 2a). The core of the Bogda anticlinorium is composed of middle-upper Carboniferous mafic intrusive rocks and volcanic strata (Allen et al., 1993; Shu et al., 2011). In the Mesozoic, the Bogda area began a stage of the continental evolution, which is evidenced by the stable sedimentary layers and lack of magmatic activity in this area (Zhu et al., 2010).

The Bogda fault zone is mainly composed of three approximately parallel faults. From south to north, these are the Erdaogou fault, Yamalike fault and Fukang fault. These faults have been thrusting northward over the Junggar basin to form an imbricated structure, and they merge into the same detachment belt in the deep crust (Wu et al., 1991). The Erdaogou fault is in the Paleozoic strata and represents the boundary between high and low mountains on the landscape. The Yamalike fault separates the Paleozoic and Cenozoic outcrops, but the topographic difference is not obvious across the fault. The range-front fault is the Fukang fault separating the Bogda mountain range from the Junggar basin. Previous studies indicate that the Fukang fault

has been the main active structure in this area since the late Quaternary (Wu et al., 2010, 2013).

The tectonic movement of the Bogda arcuate nappe structure is the most intense in the northern Tian Shan area. From Bogda peak to the piedmont alluvial plain, the elevation drops from 5445 m to approximately 1000 m, and the topographic relief is more than 4000 m over a range of 30 km from north to south (Fig. 2b).

Historically, the most destructive earthquake in the Bogda region is the 1965 *M*s 6.6 earthquake. The earthquake was attributed to the vicinity of the Erdaogou fault. Along the fault, collapses and rockfalls were observed. Approximately 30 ground fissures with consistent strikes were found near the fault (Feng, 1997). A *M*s 6.0 earthquake, located near the western edge of the Bogda arc nappe, occurred in 1934. There is no record of the earthquake damage (Fig. 2). Throughout history, the level of devastating earthquake activity in the Bogda region has not been high compared with the other regions, and the focal depths for earthquakes mainly range from 20 to 40 km (Li et al., 2004). Focal mechanism solutions show earthquakes in this region are mostly thrust events, and the principal compressive stress is in the NNE direction (Long et al., 2008).

3 Late Quaternary geomorphology of the northern Bogda piedmont

Based on a previous divisional categorization by Chen (2011), there are three main geomorphic surfaces in the northern Bogda piedmont area (Fig. 3a). Due to late Quaternary deposition in the footwall of the Fukang fault, the older geomorphic surfaces are buried. Near the Baiyang river, the three geomorphic surfaces are all present in the

hanging wall of the Fukang fault, but only one geomorphic surface can be observed in the footwall (Fig 3.b).

Fan 3: Because of the erosion on the hanging wall of the fault, the geomorphic surface Fan 3 is highly discontinuous, and it is only preserved locally along the northern Bogda piedmont. The landform surface is very flat and dips gently to the north. The geomorphic surface, which consists of the outwash and alluvial gravel (Fig. 4a), was formed in the last phase of the Dadonggou glacial period (Qiao, 1981; Han and Ye, 1985; Zhang et al., 1995). Gao and Liu (1990) estimated that the age of the gravel is 260 ka BP with the thermoluminescence (TL) dating method. The electron spin resonance (ESR) age of the bottom of the loess above the fluvial gravel is 291 ± 29 ka (Chen, 2011). Therefore, the formation time of the highest geomorphic surface in the northern Bogda piedmont is approximately 260 to 300 ka. This surface is more than 100 m higher than the piedmont alluvial fans.

Fan 2: The geomorphic surface Fan 2 is composed mainly of high terraces and older alluvial fan, and it is approximately 20 - 40 m higher than the modern river bed. There are some N-S-oriented gullies on the surface, which is covered with a loess layer (Fig. 4.b). In remote sensing images, the geomorphic surface is easily distinguished, as it is characterized by a gray-white color. In the vicinity of the Baiyang river, the geomorphic surface is approximately 30 m higher than the modern alluvial fan. The surface is mainly located in the hanging wall of the fault; it is buried in the footwall of the fault (Fig. 3).

This geomorphic surface is widely distributed in the Bogda and Urumqi area. The

^{14}C ages from the bottom of the loess are 30.6 ± 0.6 ka BP (Feng, 1997) and/or 35.9 ± 1.2 ka BP (Song et et al., 2009). You et al. (2003) presented a TL age of 49.2 ± 3.9 ka for the upper part of the gravel layer. The formation age of this geomorphic surface should be in the middle-late period of late Pleistocene, approximately 35 to 50 ka.

Fan 1: The geomorphic surface Fan 1 is widely distributed along the northern Bogda piedmont, which is composed mainly of the second terrace and alluvial fans. The fan surface is relatively flat (Fig. 4c). The TL dating results of the gravel mainly range from 15.0 ± 1.3 to 18.9 ± 1.6 ka (Wu et al., 2013). The lowermost part of the loess on the alluvial fans yields a ^{14}C age of 15.8 ± 0.2 ka, and the TL age of the uppermost part of the gravel is 27.0 ± 2.1 ka (Feng, 1997). Combined, these dating results suggest that the formation age of the surface topography is approximately 15 - 25 ka, which is consistent with previous results (Deng et al., 1991, 2000; Zhang et al., 1995).

The geometry of a geomorphic surface can record the features of tectonic deformation (Burbank and Anderson, 2012). Field investigations and interpretations of aerial photographs reveal the late Quaternary deformation of the Fukang fault. The deformation features of the geomorphic surfaces were dominated by vertical dislocation without horizontal movement. All of these findings indicate that the Fukang fault is a thrust fault. The Fukang fold and thrust belt features as an obvious inclined monocline with dips that vary between 30° and 65° to the SSW. The survey profile of the deformation terraces suggests that the fault hanging wall was mostly uplifted with no obvious fold deformation (Fig. 3c), which indicates that the tectonic style is a fault bend fold (Lave and Avouac, 2000).

4. Late Quaternary activity of the Fukang fault

4.1 Displacement characteristics of the Fukang fault

The Fukang fault, approximately 120 km in length, is composed of several secondary faults (Fig. 2). The fault dislocates the geomorphic surfaces of the northern Bogda piedmont. The displacements of the geomorphic surfaces feature different chronologies, and the dislocation is much greater in the older geomorphic surface. The vertical displacement is greater than 85 m on the Fan 3 surface, 13-31 m on the Fan 2 surface, and 3.5-6.1 m on the Fan 1 surface (Table 1). Because the geomorphic surfaces on the footwall are almost buried, the vertical displacements of the surfaces are all minimum estimates.

4.2 Kinematic characteristics of the fault

The Fukang reverse fault has varying dip angles from 10° to 40°. For example, the fault dip angle is approximately 40° at the Wugonggou river (Fig. 4d), 30° at the Jimushaer city (Fig. 4f), and only approximately 10° at the Dalonggou river (Fig. 4e).

Along the middle segment of the fault, the fault scarp on the alluvial fan is very obvious. There are two geomorphic surfaces in the eastern area of the Huangshan river (Fig. 5). The scarp height is approximately 3.5 m on the Fan 1 surface and approximately 12 m on the Fan 2 surface. The scarp strike also varies obviously, especially near the transition zone of the two geomorphic surfaces, indicating that the Fukang fault is a low-angle fault at this area.

A trench was dug on the Fan 1 surface. The trench reveals a low-angle thrust fault with a dip angle of only ~20°. The trench reveals that the stratigraphy of the two walls

is very different. The hanging wall is composed of gravel layers, whereas the footwall is composed of gravel and soil layers (Fig. 6). The layers can be divided into seven sedimentary units:

Unit ①: Grayish-yellow soil, with a small amount of angular gravel in the bottom part. This unit represents the deluvial and aeolian sedimentary facies.

Unit ②: Yellow soil, locally containing some breccia; this unit consists mainly of aeolian deposits.

Unit ③, ④: Colluvial wedge; this unit is grayish-yellow and consists of angular gravel and soil layers. The particle size of the angular gravel ranges from 2 to 5 cm and lacks bedding.

Unit ⑤: Melange layer of brown-yellow soil and black-grey angular gravel. The gravel particle size is mostly less than 1 cm; a few gravel clasts are 2 cm in diameter. The thickness of this unit is only 30-100 cm in the hanging wall but is approximately 400 cm in the footwall of the fault, and obvious bedding can be observed in the gravel layer.

Unit ⑥: Sand and gravel layer, filled by soil. This layer is yellow in general. The alluvial gravels are sub-rounded and feature horizontal bedding.

Unit ⑦: Gray gravel layer with horizontal bedding. The alluvial gravels are rounded, and the particle size of the gravels ranges mostly from 5 to 15 cm, although a few gravel clasts are 50 cm in diameter. A set of sand layers, approximately 30-40 cm in thickness, is mingled with this unit.

To accurately constrain the stratigraphic sequence, 19 optically stimulated

luminescence (OSL) samples were collected. The OSL samples were all collected from the soil or sand layers and dated in the State Key Laboratory of Earthquake Dynamics, Institute of Geology, China Earthquake Administration (CEA). We selected 4-11 μm fine-grained quartz via the pre-treatment process in a darkroom and analyzed them using the sensitivity-corrected multiple aliquot regenerative-dose (SMAR) protocol. The equivalent dose was tested with the simple multi-chip regeneration method.

The results of the OSL samples (Table 2) are consistent with the ages of the strata sequence. The unit ① is the most recent deposition on the late Holocene aged scarp. In the ② layer, the ages of the 7 samples other than the DHS-TL-04 sample ranges from 3.5 to 7 ka, which indicates this unit formed in the middle to late Holocene. The depositional duration of the unit ⑤ is very long; the age of the lower stratum is 28.21 ± 1.71 ka, and the age of the top is only approximately 7 ka. The age of the unit ⑦ is approximately 70 ka.

4.3 Slip rate of the fault

Because the piedmont alluvial fan is proximal to its source, the sediments are often very coarse and lack organic matter suitable for ^{14}C dating. Thus, the surface ages are usually determined by dating sand lenses or aeolian loess near the surface. The sand lenses are often buried a few meters beneath the surface and the aeolian loess mostly covers the fan surface; therefore, both of them cannot accurately represent the abandonment age of the surface. Due to the age uncertainty, previous studies on the late Quaternary slip rate of the Fukang fault offered a range of rates from 0.10 to 1.42 mm/yr (Luan et al., 1998; You et al., 2002, 2003). To obtain the slip rate since the late

Quaternary, we first compare the corresponding layers of the two walls of the fault, then calculate the slip rate with the typical layer displacement and the corresponding age.

In the trench, the unit ⑤ is easily distinguished because the psephicity and size of the gravels in this unit are obviously different from the other units. The time span of deposition in the unit ⑤ is very long. The OSL age of the lower part of the unit ⑤ in the hanging wall is 25.92 ± 2.25 ka, and the age of the lower part of the unit ⑤ in the footwall is 24.09 ± 1.49 to 8.21 ± 1.71 ka. The vertical displacement of the correlative horizon is approximately 4.3 m; thus, the total vertical displacement is 7.8 ± 0.5 m including the height of the surface scarp (Fig. 7). Therefore, we determine that the average vertical slip rate of 0.24-0.37 mm/yr since the late Pleistocene. The fault dip angle exposed by the trench is only 20°. If we consider material conservation and the fault bend fold model (Molnar et al., 1994; Lave and Avouac, 2000), the fault slip rate (s), the vertical slip rate (v) and the fault dip (θ) can be formulated approximately as $s=v/\sin\theta$. Using this equation, we obtain a fault slip rate of 0.71-1.10 mm/yr. The Fukang fault is a listric shape, and the fault merges into a nearly horizontal detachment at depth (Wu et al., 1991). Thus, the crustal shortening rate is approximately 0.90 ± 0.20 mm/yr. GPS data show that the N-S crustal shortening rate is approximately 2-5 mm/yr in the eastern Tian Shan (Abdrakhmatov et al., 1996; Zhang et al., 2002; Yang et al., 2008). Several active fault zones in the eastern Tian Shan have been demonstrated to absorb the crustal shortening deformation, and the crustal shortening rate in the Bogda area is only 1-2 mm/yr (Li et al., 2010; Yang et al., 2008).

5 Discussion

5.1 Displacement distribution and slip model of the Fukang fault

The activity of the Fukang fault has been very intense since the late Quaternary. The fault dislocated the geomorphic surfaces in the northern piedmont of the Bogda. We surveyed the vertical displacement of the fault on the different geomorphic surfaces (Fig. 8). The distribution of the displacements can reflect the long-term characteristics of fault movement (Burbank and Anderson, 2012).

On the youngest geomorphic surface (Fan 1), we did not observe an obvious trend in the distribution of the fault displacement because the surface is too young. The envelope of the displacements has some fluctuations, which probably indicates that there are several rupture segments along the Fukang fault. The trench revealed that the previous coseismic displacements are different at the same location (You et al., 2002), and the recurrence interval ranges from 1.5 ka (You et al., 2003) to 3.75 ka (Wu et al., 2013). On the Fan 2 and Fan 3 surfaces, although the displacement data are limited, the distribution characteristics of the fault displacements are similar. The position of the maximum displacement is located at 35-40 km along the fault, and the vertical displacements decrease gradually towards both sides, showing an asymmetric normal distribution (Fig. 8). The slip rate of the fault is thus larger in the middle segment and gradually decreases towards both sides (You et al., 2002), which is consistent with the distribution characteristics of the fault displacement. The Fukang fault deformation characteristics may be in agreement with the fault growth development model described by Cartwright et al. (1995). The position of the maximum vertical

displacement of the fault is also consistent with the location of Bogda peak, which indicates that the long-term fault movement controls the relief development of the range. According to the displacement distribution and the paleoearthquake research on the fault, we consider that the rupture characteristics of the Fukang fault during the late Quaternary may be belong to the Variable-slip Model.

5.2 Deformation process of the Bogda nappe structure

Since the Cenozoic, the Tian Shan has experienced several periods of rapid uplift (Hendrix et al., 1994; Deng et al., 2000; Liu et al., 2004; Wang et al., 2008). The appearance of growth strata and an angular unconformity in the foreland basin (Bullen et al., 2001; Chen et al., 2002) represents the beginning of piedmont deformation due to the thrusting and folding (Fu et al., 2003). In the piedmont area, there are several rows of fault and fold belts whose activity has migrated from mountain to basin. The second row of tectonic belts formed in the late Pliocene to early Pleistocene and peaked at the end of the early Pleistocene (Deng et al., 2000). The frontal reverse fault-fold belt began to be deformed during the early Middle Pleistocene, then uplifted rapidly during the middle to late periods of the Middle Pleistocene (Deng et al., 2000).

Low-temperature thermochronology studies (Liu et al., 2004; Wang et al., 2008) have shown that the Bogda range has experienced the same tectonic uplift history. The Fukang fault in the northern piedmont of the Bogda range may have controlled the Cenozoic sedimentary history in this area. The thickness of the Cenozoic sediments in the footwall of the fault is approximately 2000 m (Wu et al., 2004). In the area south of the Fukang fault, Mesozoic and Paleozoic strata are widely distributed (Fig. 2), which

indicates that the Fukang fault has been continuously active as a boundary fault of the Bogda mountain range since the Cenozoic. Although the Beisantai anticline has been uplifted in the Junggar basin (Fig. 2), the length of the anticline is only approximately 15 km, and the maximum uplift amplitude is approximately 70 m. The tectonic deformation of the Bogda area remains mainly concentrated in the Fukang fault zone. We observed that the new activity of the fault does not obviously migrate to the north, and this is different than the behavior of the other nappe structures of the Tian Shan.

5.3 Characteristics of the tectonic uplift in the Bogda area

The remote effects of the India-Eurasia collision during the Cenozoic have led to rapid uplift of the Bogda mountain range (Tapponnier and Molnar, 1977; Avouac et a1., 1993). The crustal shortening rate of this area during the late Quaternary is only approximately 1 mm/yr. The crustal shortening rate of the Bogda range is much less than the rate of 3-5 mm/yr observed along the western segment of the northern Tian Shan (Deng et al., 2000; Yang et al., 2008). However, the uplift magnitude of the Bogda range is more than that of the western Tian Shan area; thus, the Bogda range has a peak elevation of 5445 m in the northern Tian Shan mountains.

Although the Fukang fault dips only approximately 20° near the surface, petroleum geophysical profiles show that the fault has a listric shape at depth and belongs to the thick-skinned nappe structure (Wu et al., 1991). The distance between the frontal fault and the root fault of the Bogda nappe is approximately 13-18 km, and the earthquake focal depth of this area is 20-40 km (Li et al., 2004). If the depth of the detachment zone is 20 km, the Fukang fault dip angle is approximately 50°. The seismic profiles also

confirm that the fault dip angle is more than 45° (Wu et al., 2004). Therefore, the vertical uplift rate along the fault is 0.54-0.85 mm/yr. The low-temperature thermochronology research suggests that rapid uplift of the Bogda range began at 3-5 Ma (Wang et al., 2008). With the vertical uplift rate, we roughly estimate that the magnitude of uplift since the Pliocene is more than 4000 m. This height is consistent with the modern geomorphology of the Bogda area.

The deep structure has obvious difference between the western segment of the northern Tian Shan and the Bogda area. To the west of Urumqi, it is a thin-skinned nappe structure (Avouac et al., 1993; Liu et al., 1994; Deng et al., 2000) characterized by a gently dipping detachment and deformation propagating towards the basin. The frontal belt of the nappe has propagated approximately 40-50 km towards the basin (Fig. 9). The crustal shortening rate of the western segment of northern Tian Shan is 3-5 mm/yr (Deng et al., 2000; Yang et al., 2008), which is significantly higher than that of the Bogda area. However, the deformation of this region is characterized by propagation towards the basin, and the vertical uplift is limited. The tectonic deformation can be considered lateral growth.

The thickness of the Cenozoic sediment in the Bogda area is only approximately 2000 m (Wu et al., 2004). The layers of the northern Bogda piedmont are composed of resistant Paleozoic strata; thus, the tectonic belt is narrower and tighter than that of the western segment, and the propagation deformation towards the basin is very limited. The Bogda fault zone is a typical thick-skinned nappe structure. The tectonic deformation along the Bogda range can be considered vertical growth. Although the deformation rate

is small, the uplift amplitude is very significant in this region (Fig. 9).

6. Conclusions

The Fukang fault in the northern piedmont of the Bogda range has been continuously active since the Cenozoic as a boundary fault of the Bogda mountain range. The tectonic deformation of the Bogda region has been mainly concentrated in the Fukang fault zone during the late Quaternary. A low dip angle thrust, the Fukang fault, is present near the surface, and the average crustal shortening rate of the fault has been 0.90 ± 0.20 mm/yr since the late Quaternary.

Based the 32 displacement surveys on different geomorphic surfaces, we concluded that the rupture characteristics of the Fukang fault during the late Quaternary belong to the Variable-slip Model. The kinematic characteristics of the fault also correspond to the landscape of the Bogda mountain range over long time scales.

The Bogda nappe is a thick-skinned structure. The fault has a listric shape at depth, and a steep thrust fault separates the Bogda range and the foreland basin. The Bogda tectonic belt is much tighter, and deformation propagates slightly towards the basin. The deformation characteristics of this region feature vertical uplift. Although the deformation rate is small, the uplift amplitude is very significant in this region.

Acknowledgements

The author appreciates Professor W. Zheng and H. Zhang for their helpful discussion. This research is supported by National Natural Science Foundation of China (41102137, 41372220, 41172194), National Key Laboratory of Earthquake

Dynamics Fund (LE1413) and the Ministry of Finance major projects "An earthquake surveillance and protection zone of active faults seismic risk evaluation".

References

Abdrakhmatov, K. Y., Aldazhanov, S. A., Hager, B. H., Hamburger, M. W., Herring, T. A., Kalabaev, K. B., 1996. Relatively recent construction of the tien shan inferred from GPS measurements of present-day crustal deformation rates. Nature, 384(6608), 450-453.

Allen, M.B., Windley, B. F., Zhang, C., 1993. Paleozoic collisional tectonics and magmatism of the Chinese Tien Shan, central Asia. Tectonophysics, 220, 89-115.

Allen, M.B., Vincent, S. J., Wheeler, P. J., 1999. Late Cenozoic tectonics of the Kepingtage thrust zone: Interactions of the Tien Shan and Tarim Basin, Northwest China. Tectonics, 18(4), 639-654.

Avouac, J. P., Tapponnier, P., Bai, M., You, H., Wang, G., 1993. Active faulting and folding in the northern Tian Shan and rotation of Tarim relative to Dzungarian and Kazakhstan. Journal of Geophysical Research, 98(4), 6755-6804.

Bullen, M. E., Brubank, D. W., Garver, J. I., Abdrakhmatov, K. Y., 2001. Late Cenozoic tectonic evolution of the northwestern Tien Shan: New age estimates for the initiation of mountain building. Geological Society of America Bulletin, 113(12), 1544-1559.

Bullen, M. E., Burbank, D. W., Garver, J. I., 2003. Building the northern Tien Shan: Integrated thermal structural, and topographic constraints. Journal of Geology, 111, 149-165.

Burbank, D. W., McLean, J. K., Bullen, M., Abdrakhmatov, K. Y., Miller, M. M., 1999. Thrust-belt partitioning of intermontane basins by basement folding, Tien Shan, Kyrgyzstan. Basin Research, 11, 75-92.

Burbank, D. W., Anderson, R. S., 2012. Tectonic geomorphology. Wiley-Blackwell Science, Oxford, pp17.

Burchfiel, B., Brown, E. T., Deng, Q ., Feng, X., Li, J., Molnar, P., Shi, J., Wu, Z., You, H., 1999. Crustal shortening on the margins of the Tien Shan, Xinjiang, China. International Geology Review, 41(8)：665-700.

Cartwright, J. A., Trudgill, B. D., Mansfield, C. S., 1995. Fault growth by segment linkage: an explanation for scatter in maximum displacement and trace length data from the Canyonlands grabens of SE Utah. Journal of structural geology, 17, 1319-1326.

Chen, L., 2011. Late Quaternary behavior of the atcive tectonic system in the Urmuqi transform region of the North Tianshan. Doctoral dissertation of Institute of Geology, CEA, pp66-68.

Chen, J., Burbank, D.W., Scharer, K. M., Sobel, E., Yin, J., Rubin, C., Zhao, R., 2002. Magnetochronology of the upper Cenozoic strata in the southwestern Chinese Tian Shan: Rates of Pleistocene folding and thrusting. Earth &Plantary Science Letters, 195 (1-2), 113-130.

Deng, Q., Feng, X., You, H., Chen, J., Li, J., Zhang, Y., Xu, X., Wu, Z., Zhang, H., 1991. Paleoseismology and late Quaternary activity of the Dushanzi-Anjihai reverse fault zone, Xinjiang. Research of Active Fault, 1, 37-55(in Chinese with

English abstract).

Deng, Q., Yu, G., Ye, W., 1992. Study on the relationship of earthquake surface rupture parameters and magnitude. *Research onActive Faults*, Seismological Press, Beijing, (2):247-264 (in Chinese with English abstract).

Deng, Q., Feng, X., Zhang, P., Xu, X., Yang, X., Peng, S., Li, J., 2000. Active Tectonics of Tianshan. Seismological Press, Beijing, pp302-321 (in Chinese).

Feng, X., 1997. The paleoearthquakes in Xinjiang region. Sci-Tech and Public Health Press of Xinjiang, Urumqi (in Chinese).

Fu, B., Lin, A., Kano, K., Maruyama, T., Guo, J., 2003. Quaternary folding of the eastern Tian Shan, northwest China. Tectonophysic, 369, 79-101.

Gao, C., Liu, J., 1990. Study on loess along the Urumqi River Valley. Quaternary Research, 3, 251-260 (in Chinese with English abstract).

Ghose, S., Hamburger, M. W., Ammon, C. J., 1998. Source parameters of moderate-sized earthquakes in the Tien Shan, Central Asia from regional moment tensor inversion. Geophysical Research Letters, 25(16), 3181-3184.

Han,S., Ye, W., 1985. The late Pleistocene deposit environment in Cangfanggou of Urumqi. Collection of Quaternary Study in Arid Xinjiang. Urumqi: Xinjiang People′s Press, 21-31 (in Chinese).

Hendrix, M.S., Dumitrn, T.A., Graham, S.A., 1994. Late Oligocene-Early Miocene unroofing in the Chinese Tianshan: An earlyeffect of the India-Asia collision. Geology, 22(6), 487-490.

Lave, J., Avouac, J.P., 2000. Active folding of fluvial terraces across the Siwaliks Hills,

Himalayas of central Nepal. Journal of Geophysical Research, 105, 5735–5770.

Li, J., Wang, X., Tan, K., Liu, D., Pa, H., Jiang, J., Fang, W., 2010. Analysis of movement characters of present-day active tectonics of northern Tianshan region. Journal of Geodesy and Geodynamics, 30(6), 1-5 (in Chinese with English abstract).

Li, T., Wang, Z., Zhou G., Liu, Y., Li, Y., 2004. The segmentation and the relationship between shallow and deep structures of Bogda Mountain, Xinjiang, Northwest China. Earth Science Frontiers, 11(3), 103-114 (in Chinese with English abstract).

Liu, H., Liang, H., Cai L., Xia, Y., Liu, L., 1994. Evolution and structural style of Tianshan and adjacent basins, northwestern China. Earth Science-Journal of China University of Geosciences, 19(6), 727-741 (in Chinese with English abstract).

Liu, Y., Wang, Z., Jin, X., Li, T., Li, Y., 2004. Evolution, chronology and depositional effect of uplifting in the eastern sector of the Tianshan Mountains. Acta Geologica Sinica, 78(3), 32-44.

Long, H., Gao, G., Nie X., Li, Y., Shen, J., 2008. The focal mechanism solution and stress field inversion of small and moderate earthquakes along middleeastern part of northern Tianshan Reion. Earthquake, 28(1), 93-99 (in Chinese with English abstract).

Lü, H., Li, Y., Nan, F., Si, S., Liu, Y., Qian, M., Zhao, H., 2008. Sequences and ages of fluvial terraces along the northern piedmont of the Tianshan Mountains. Acta Geographica Sinica. 63(1), 65-74(in Chinese with English abstract).

Luan, C., Hu, J., Luo, F., Li, M., Hu, W., 1998. The structures and activities in Holocene on the western segments of northern Bogeda Fault in Xinjiang. Inland Earthquake , **12**(4), 355-361.

Molnar, P., Tapponnier, P., 1975. Cenozoic tectonics of Asia: Effects of a continental collision: Features of recent continental tectonics in Asia can be interpreted as results of the India-Eurasia collision. Science, 189(4201), 419-426.

Qiao, Z., 1981. The outline of Quaternary layers in Urumqi River and Toutun River Drainage Area. Collection Papers of Quaternary Geology and Glacier of Xinjiang, Xinjiang People's Press, Urumqi, 176-183 (in Chinese).

Reigber, C., Michel, G. W., Galas, R., Angermann, D., Klotz, J., Chen, J., Papschev, A., Arslanov, R., Tzurkov, V. E., Ishanov, M. C., 2001. New space geodetic constrains on the distribution of deformation in Central Asia. Earth Planetary Science Letters, 191, 157-165.

Shen, C., Mei, L., Liu, L., Tang, J., Zhou, F., 2006. Evidence from apatite and zircon fission track analysis for Mesozoic-Cenozoic uplift thermal history of Bogeda Mountain of Xinjiang, northwest China. Marine Geology&Quaternary Geology, 26(3), 87-92 (in Chinese with English abstract).

Shu, L., Wang, B., Zhu, W., Guo, Z., Charvet, J., Zhang, Y., 2011. Timing ofinitiation of extension in the Tianshan, based on structural, geochemical and geochronological analyses of bimodal volcanism and olistostrome in the Bogda Shan(NW China). International Journal of Earth Sciences, 100(2), 1647-1663.

Song, H., Shen, J., Xiang, Z., Li, J., Rou, J., 2009. The active fault detecting and

seismic risk assessment in Urumqi city. Seismological Press, Beijing, pp155-159 (in Chinese).

Tapponnier, P., Molnar, P., 1979. Active faulting and Cenozoic tectonics of the Tien Shan, Mongolia, and Baykal regions. Journal of Geophysical Research, 84, 3245-3459.

Wang, Q., Li, S., Du, Z., 2009. Differential uplift of the Chinese Tianshan since the Crctaceous: Constraints from sedimentary petrography and apatite fission-track dating. International Journal of Earth Sciences, 98(6), 1341-1363.

Wang, Q., Zhang, P., Niu, Z., Freymueller, J. F., Lai, X., Li, Y., Zhu, W., Liu, J., Bilham, R., Larson, K. M., 2002. Present-day crustal movement and tectonic deformation in China continent. Science in China (Series D), 45 (10), 865-874.

Wu, C., Shen, J., Shi, J., Luo, F., Chen, J., 2010. Late-Quaternary Activity of the Gumudi Fault of the South Fukang Fault Belt on the North Margin of the Bogda Mountains in the Xinjiang Automonous Regin. Quaternary Sciences, 30(5), 1020-1029 (in Chinese with English abstract).

Wu, C., Chen, J., Shen, J., Song, H., Wu, G., Luo, F., 2013. Late-Quaternary Activity Characteristic of the Ganhezi Segment of the Fukang Fault Belt, in Xinjiang. Earth Science-Journal of China University of Geoscience, 38(3), 632-640(in Chinese with English abstract).

Wu, K., Cha, M., Qu, J., Tian, H., 2004. Control of Bogeda Mountain uplift on the structural formation and evolution in Beisantai region. Journal of China University of Petroleum(Edition of Natural Science), 28(2), 1-5(in Chinese with

English abstract).

Wu, Z., Guo, F., 1991. Second discussion of Bogda nappe tectonic and its oil-gas accumulation. Xinjiang Geology, **9**(1), 40-49(in Chinese with English abstract).

Yang, S., Li, J., Wang, Q., 2008. The deformation pattern and fault rate in the Tianshan Mountains inferred form GPS boservations. Science in China (Series D), 51(8), 1064-1080(in Chinese).

Yin, A., Nie, S., Craig, P., Harrison, T. M., 1998. Late Cenozoic tectonic evolution ofthe southern Chinese Tian Shan. Tectonics, 17(1), 1-27.

You, H., Ren, L., Chen, G., Wang, W., 2002. Activity forms and slip rates of Fukang fault. Earthquake Research in China, **18**(3), 239-248 (in Chinese with English abstract).

You, H., Ren, L., Zhang, Y., 2003. Structural geometry and activities of the Fukang-Jimsar fualt zone, Xinjiang. Seismology and Geology, **25**(3), 375-384 (in Chinese with English abstract).

Zhang, P., 2003. Late Cenozoic tectonic deformation of Tianshan mountain and its foreland basin. Chinese Science Bulletin, 48(24), 249-250 (in Chinese).

Zhang, P., Wang, M., Gan, W., Deng, Q., 2003. Slip rates along major active faults from GPS measurements and constraints on contemporary continental tectonics[J]. Earth Science Frontiers, 10(special issue), 8l-92 (in Chinese with English abstract).

Zhang, P., Deng, Q., Yang, X., Peng, S., Xu, X., Feng, X., 1996. Late Cenozoic tectonic deformation and mechanism along the Tianshan Mountain,North

Western China. Earthquake Research in China, 12 (2), 127-140(in Chinese with English abstract).

Zhang, P., Deng, Q., Yang, X., Feng, X., Peng, S., Zhao, R., 1995. Glaciofluvial geomorphology and neotectonics along the range-front of the northern Tianshan. Research on Active Faults, 4, 63-78 (in Chinese with English abstract).

Zhu, Z., Ji, J., Xu, Q., Wang, L., Sun, D., Gong, J., Zhao, L., 2010. The Late Cenozoic transpressional deformation and uplift of Bogda-Harlic Mountains. Chinese Journal of Geology, 45(3),653-665(in Chinese with English abstract).

Zubovich, A.V., Wang, X., Yuri, G.S., Schelochkov, G. G., Reilinger, R., Reigber, C., Mosienko, O. I., Molnar, P., Michajljow, W., Makarov, V. I., Li, J., Kuzikov, S. I., Herring, T. A., Hamburger, M. W., Hager, B. H., Dang, Y., Bragin, V. D., Beisenbaev, R. T., 2010. GPS velocity field for the Tien Shan and surrounding regions. Tectonics, 29, TC6014, doi:10.1029/2010TC00 2772.

Figure and table captions

Figure 1. Major cities, active faults and historic earthquakes in the Tian Shan mountains. Some major faults within the mountains: TF fault=Talas-Fergana fault, Dh fault=Dzhalair fault, Bo fault=Borohoro fault, Dz=Dzhungarian fault, KR fault=Kashi-River fault, Na fault=Nalati fault, QT fault=Qiuli-Tage fault, KT fault=Kalpin-Tage fault, STS fault= Southern TianShan fault.

Fig. 2. The geologic structure map of the Bogda region

(a) The distribution of faults and earthquakes in the Bogda region. Active faults and earthquakes are mainly located in the northern piedmont area of the Bogda

mountains. The thick red lines represent the Holocene active faults, and the thick black lines represent the late Pleistocene active faults. (b). The topographical and geological profile of the northern Bogda piedmont area. The elevation decreases from 5445 m to approximately 1000 m from south to north, and three approximately parallel faults from an imbricated structure.

Fig. 3. Distribution characteristics of the geomorphic surfaces in the northern Bogda piedmont area

3.a There are three main geomorphic surfaces in the northern Bogda piedmont area. 3.b Near the Baiyang river, the three geomorphic surfaces are all developed on the hanging wall of the Fukang fault, but only the Fan 1 geomorphic surface can be observed in the footwall. 3.c The survey profile of the deformation terraces suggests that overall uplift dominates the hanging wall of the Fukang fault.

Fig. 4 Geomorphic surface along the Bogda Mountains piedmont and Fukang fault section

4.a Fan 3 topographic surface on the hanging wall of the fault. 4.b The loess overlying the alluvial fan along the northern Bogda piedmont. 4.c Deformation of the Fan 1 geomorphic surface. 4.d Fault profile at the Wugonggou river. 4.e Low dip angle fault section near the Dalongkou river. 4.f Fault dislocating the loess in Jimushar.

Fig. 5 Measured deformation map of the alluvial fan

The red line represents the Fukang fault and the black box represents the site of the trench. a and b represent the sites of the fault scarps.

Fig. 6. Fault profile of the Dahuangshan trench

Fig. 7 Superposition map of the trench profile and the surface scarp

The black coarse line represents the surface measured by the ATK; the dotted lines represent the hypothetical site of the marker layer.

Fig. 8 Distribution of the displacements on the different geomorphic surfaces along the strike of the fault

Fig. 9 Schematic diagram of the deep tectonic model of the northern Tian Shan

9.a The western segment of the northern Tian Shan is a thin-skinned nappe structure characterized by a gently dipping detachment and deformation propagating towards the basin. 9.b The Bogda area is a thick-skinned nappe structure characterized by narrow and tight tectonic belts, and the deformation of this region is characterized by vertical uplift.

Table 1 Vertical displacements of the Fukang fault

Table 2 OSL samples dating results for the layers in the Dahuangshan trench

Table.1

Dislocated landform surface	Measuring site	Vertical displacement
Fan1	Dahonggou	5.4±0.3m
	Xiaohonggou	4.4±0.3 m
	Wugonggou	4.5±0.2 m
	Wugonggou	3.9±0.2 m
	Dalonggou	5.1±0.4 m
	Shagou	3.5±0.3 m
	Honggou	3.8±0.2 m
	Honggou	4.8±0.3 m
	Baiyang river	3.7±0.4 m
	Xigou	6.1±0.3 m
	Xigou	5.1±0.2 m
	Huangshan river	5.2±0.3 m
	Quanquangou	4.6±0.3 m
	Sheyaozigou	5.2±0.4 m
	Shuangcha river	4.5±0.3 m
	Dalongkou	6.1±0.4 m
	Dongjiangou	6.5±0.5 m
Fan2	Xiaohonggou	16.0±1.7 m
	Baiyang river	25.0±2.5 m
	Quanquangou	31.0±3.0m
	Ergonggou	26.0±2.0 m
	Ganhezi	20.0±1.8 m
	Shuangcha river	17.0±1.5 m
	Shuangcha river	16.0±1.4 m
	Shichanggou	14.5±1.5 m
	Shichanggou	13.0±1.2 m
Fan3	Jimushaer	105±5 m
	Xigou	160±6 m
	Shizhuanggou	140±4 m
	Ganhezi	95±5 m
	Shuimogou	92±4 m
	Xiaohonggou	85±5 m

Table. 2

Sample	Depth /(cm)	Moisture content	Total count rate of α (Cpks)	K （%）	Environmental dose rate (Gy/ka)	Equivalent dose (De/Gy)	OSL age (ka B.P.)
DHS-TL-01	20	0.46%	8.9±0.3	1.94	4.11±0.14	7.8±0.5	1.90±0.14
DHS-TL-02	50	2.26%	9.3±0.2	1.87	4.00±0.14	15.0±0.3	3.75±0.18
DHS-TL-03	80	2.03%	8.5±0.2	1.99	3.95±0.13	18.3±0.6	4.64±0.24
DHS-TL-04	80	1.50%	8.2±0.2	1.81	3.75±0.13	37.4±1.2	10.04±0.51
DHS-TL-05	100	0.62%	8.5±0.2	1.91	3.95±0.14	27.5±0.9	6.97±0.37
DHS-TL-06	110	0.77%	10.5±0.3	1.97	4.39±0.17	24.3±0.9	5.54±0.32
DHS-TL-07	120	1.46%	10.7±0.3	1.85	4.27±0.17	24.8±0.8	5.82±0.32
DHS-TL-08	140	1.52%	10.1±0.3	1.98	4.10±0.16	23.8±1.1	5.81±0.37
DHS-TL-09	160	1.40%	8.2±0.2	1.82	3.71±0.13	32.6±0.5	8.78±0.38
DHS-TL-10	180	0.39%	10.1±0.3	1.81	4.14±0.16	78.2±1.6	18.88±0.91
DHS-TL-11	510	3.20%	9.7±0.3	1.82	3.86±0.15	89.7±2.3	23.22±1.25
DHS-TL-12	50	3.99%	8.7±0.3	1.74	3.67±0.14	50.6±2.1	13.77±0.87
DHS-TL-13	320	1.64%	9.9±0.3	1.74	3.93±0.16	275.0±45.9	69.95±12.11
DHS-OSL-01	240	1.61%	10.7±0.4	1.82	4.20±0.17	101.1±4.2	24.09±1.49
DHS-OSL-02	250	0.44%	10.2±0.3	1.73	4.06±0.16	114.5±4.7	28.21±1.71
DHS-OSL-03	90	0.31%	10.4±0.3	1.81	4.24±0.17	109.8±8.2	25.92±2.25
DHG-OSL-04	80	2.44%	9.35±0.24	1.8	3.91±0.14	13.56±0.30	3.47±0.17
DHG-OSL-05	120	3.32%	7.73±0.22	1.86	3.59±0.12	22.38±0.61	6.24±0.32
DHG-OSL-06	150	2.50%	8.87±0.25	1.81	3.80±0.14	26.12±0.35	6.88±0.32

Figure1

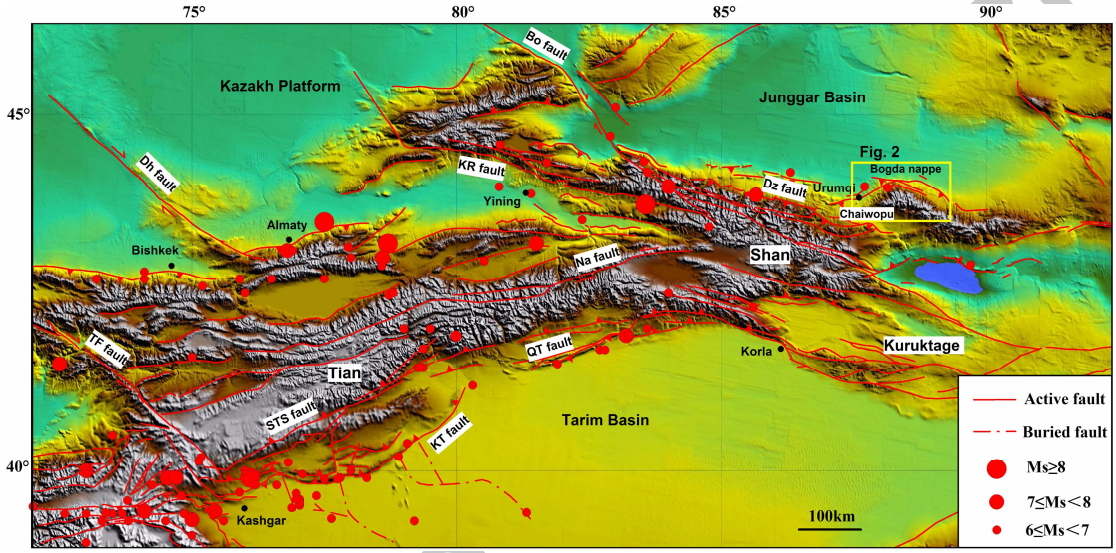

Figure2

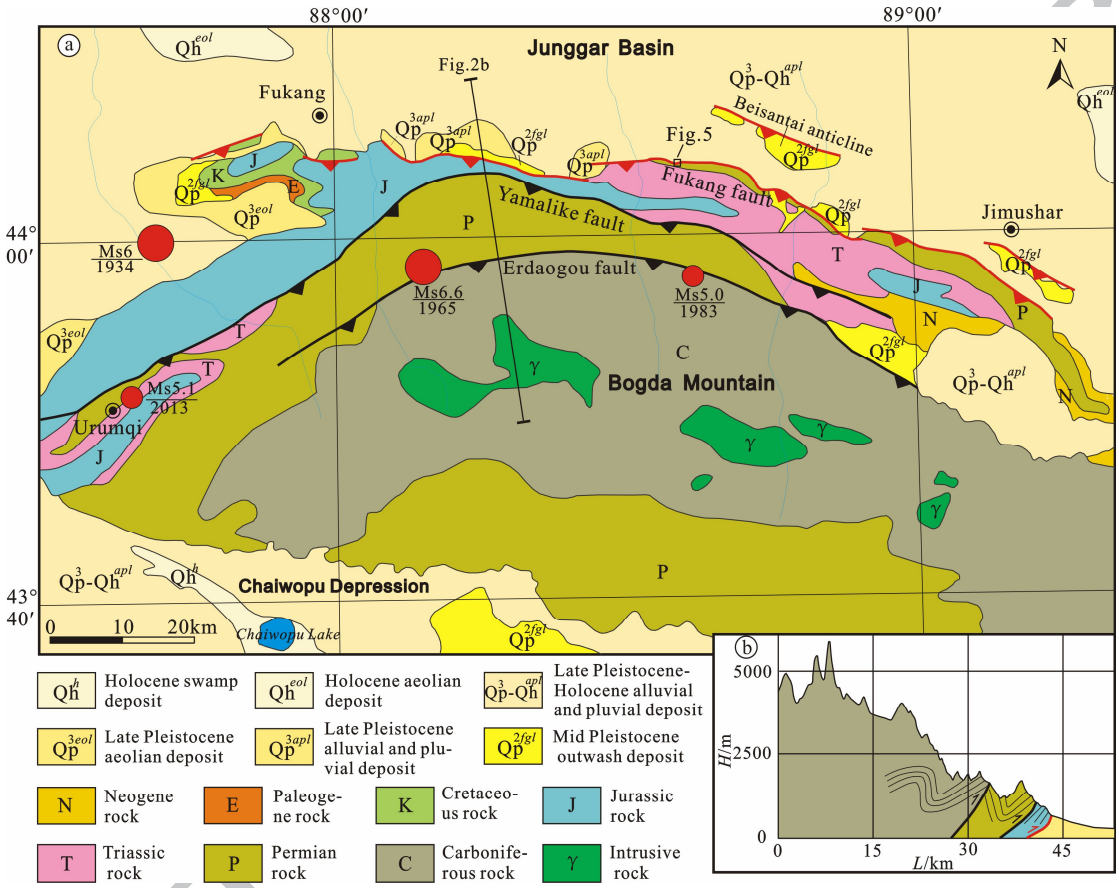

Figure3

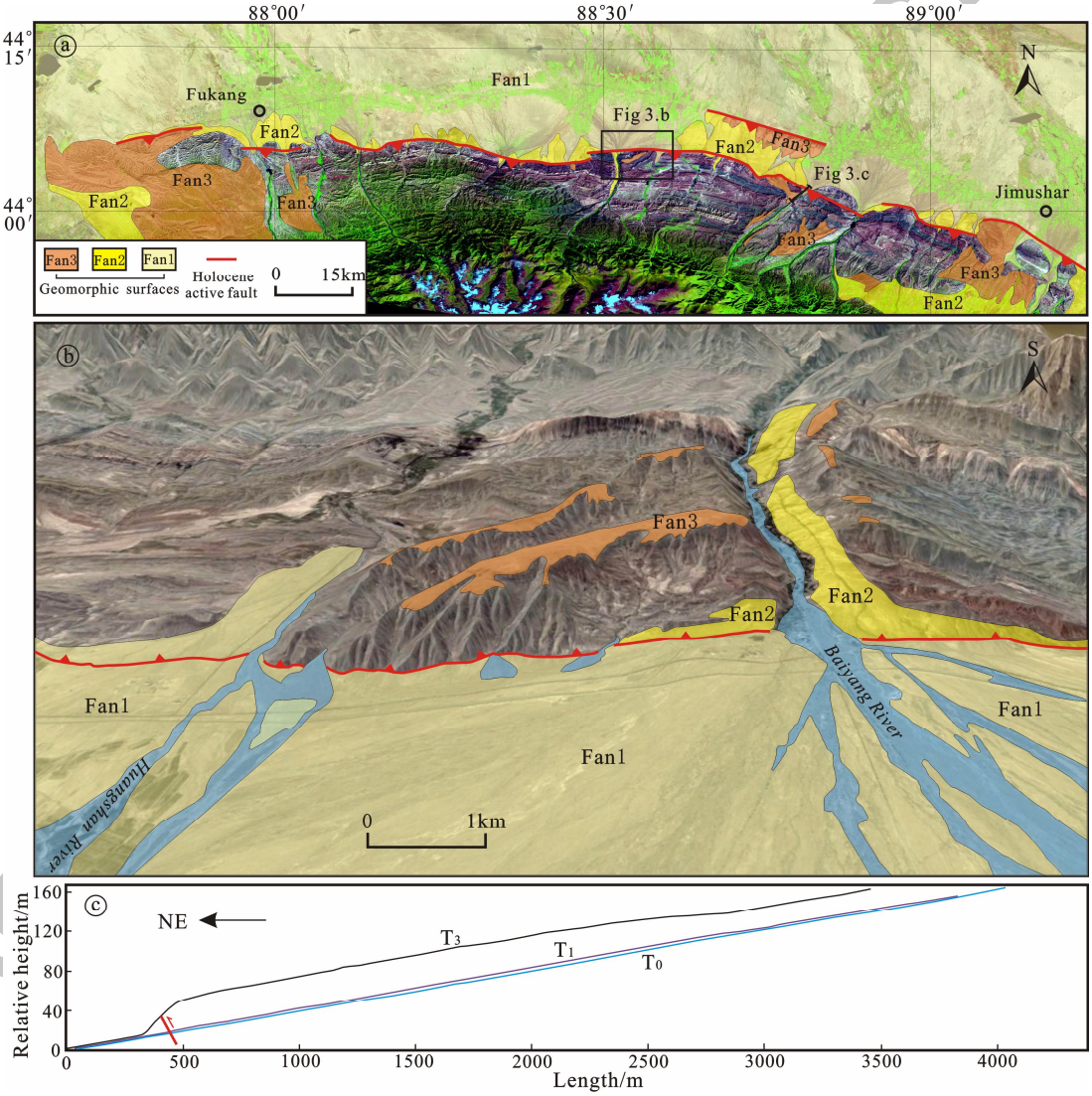

Figure4

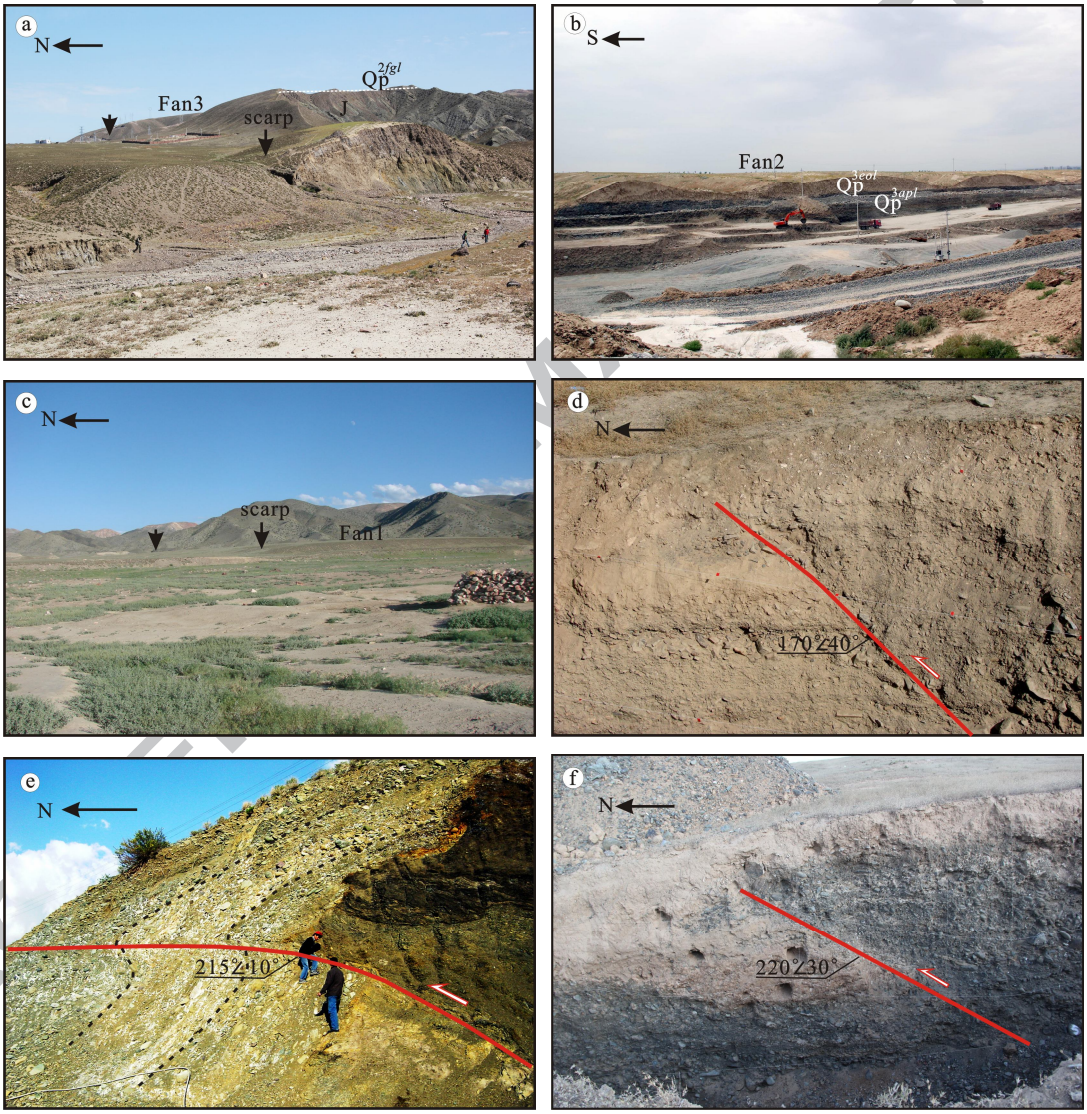

Figure5

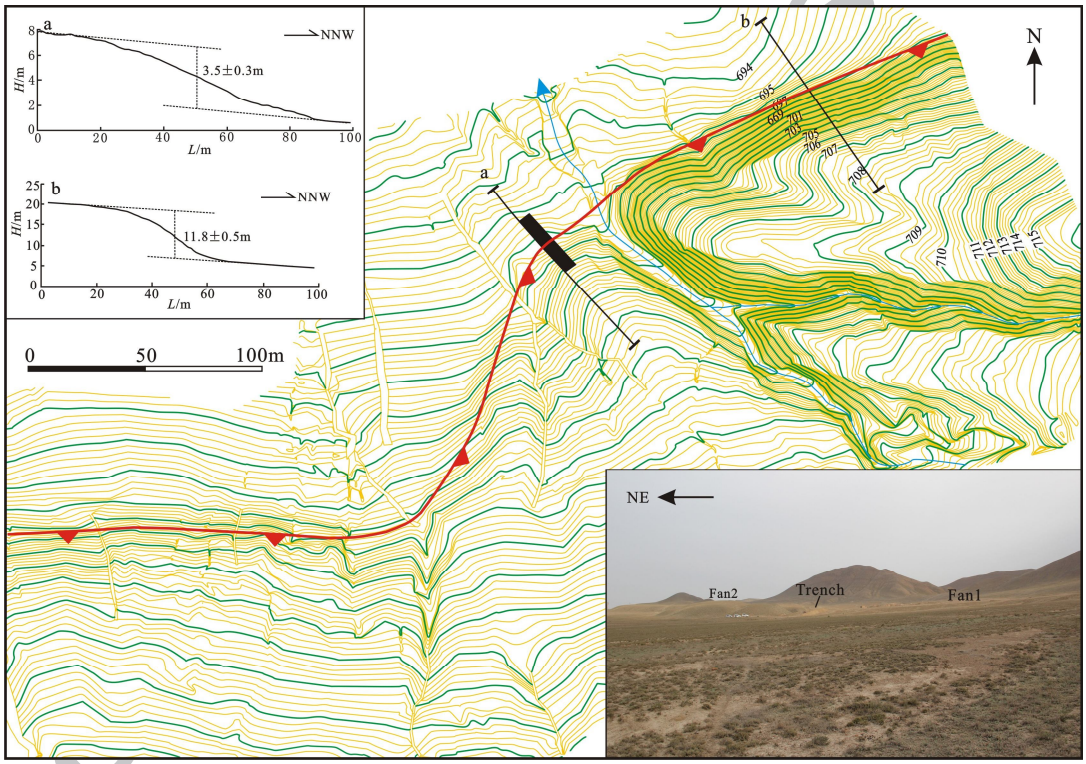

Figure6

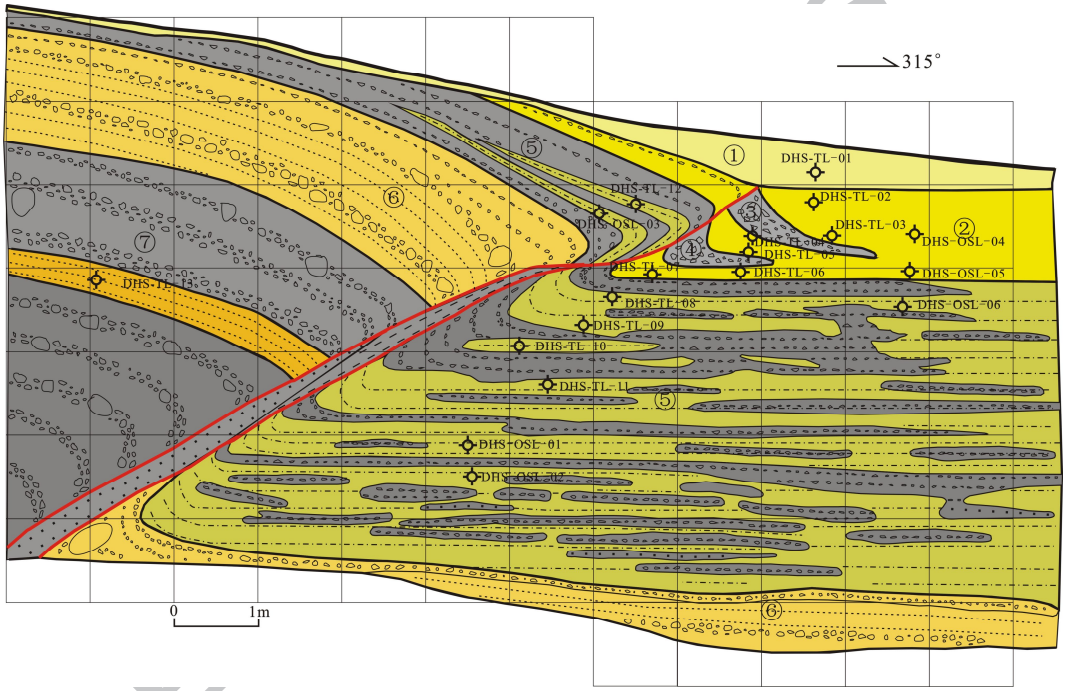

Figure7

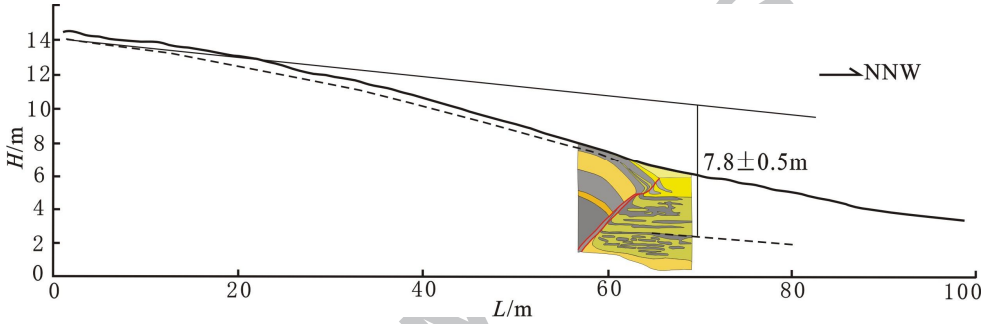

Figure8

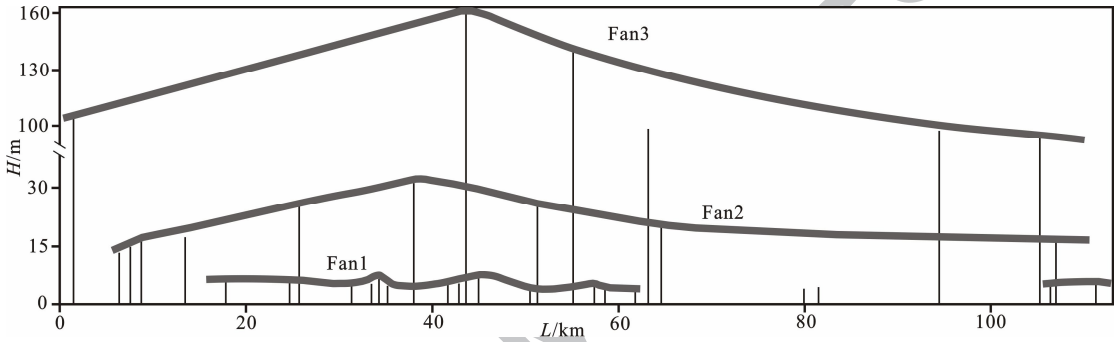

Figure9

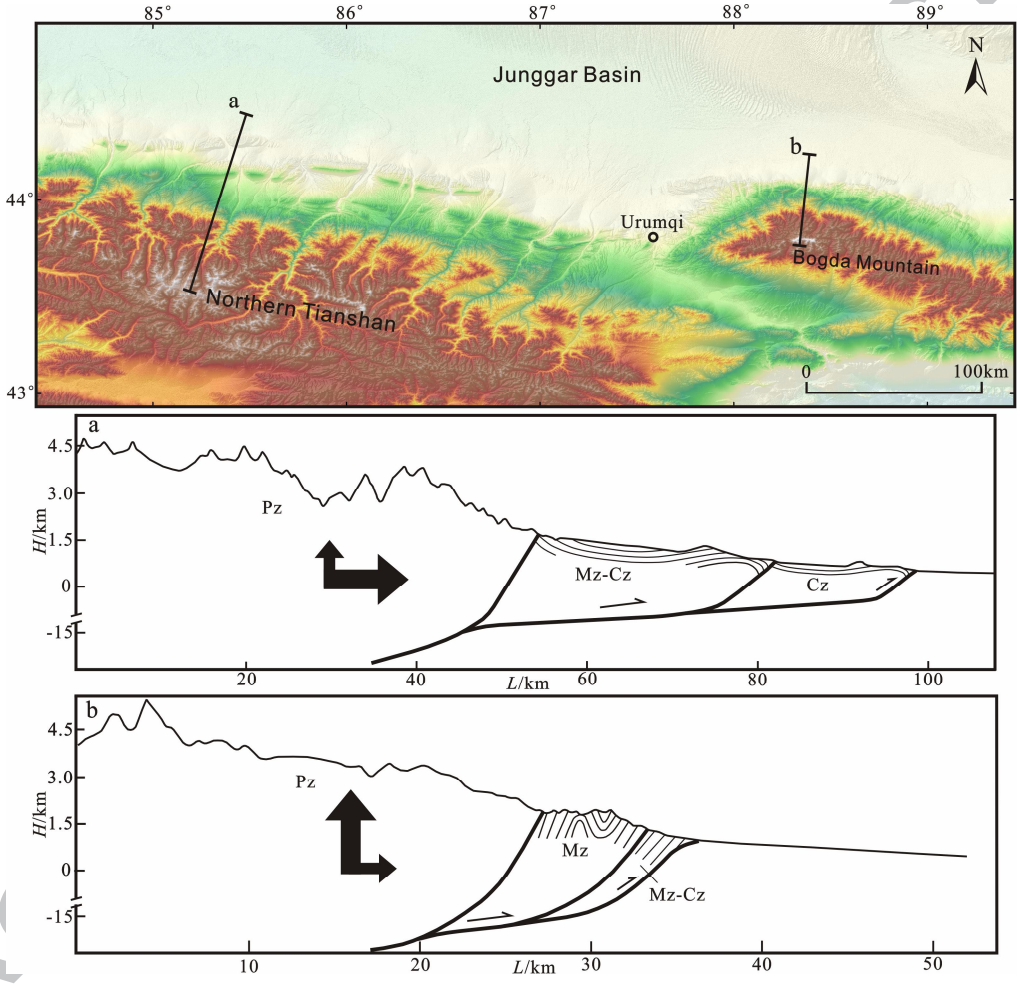

Highlights

(1) The crustal shortening rate of the Fukang reverse fault is 0.90±0.20 mm/yr.

(2) The geomorphic surfaces in the Bogda northern piedmont area are divided.

(3) The deformation characteristic of the Bogda nappe represents the vertical uplift. Although the deformation rate is small, but the uplift amplitude is very significantly in this region.